Supporting Information

Fast mass transport-assisted convective heat transfer through the multi-walled carbon nanotube array

Wonjae Jeon[a,‡], *Taehun Kim*[b,‡], *Sung-Min Kim*[b*] *and Seunghyun Baik*[b,c*]

[a]Institute of Advanced Machinery and Technology, Sungkyunkwan University, Suwon 16419, Korea.

[b]School of Mechanical Engineering, Sungkyunkwan University, Suwon 16419, Korea.

[c]Center for Integrated Nanostructure Physics, Institute for Basic Science (IBS), Suwon 16419. Korea.

*E-mail: smkim@skku.edu, sbaik@me.skku.ac.kr

‡W.J. and T.K. contributed equally to this research work.

Characterization of the VAMWNTs

The mass (M_{VAMWNT}) and volume (V_{VAMWNT}) of each nanotube were characterized following a previously published protocol.[S1-3] The inner ($d_{int} = 7.0\ nm$) and outer ($d_{out} = 11.4\ nm$) diameters of nanotubes were measured using scanning electron microscopy (SEM) and transmission electron microscopy (TEM) images. The average number of walls (n) was 5. M_{VAMWNT} and V_{VAMWNT} were calculated using following equations. [S1-3]

$$M_{VAMWNT} = \frac{1}{1315}\pi\tau L\left[nd_{int} + 2d_{s-s}\sum_{i=0}^{n-1} i\right] \qquad \text{(S1)}$$

$$V_{VAMWNT} = \pi\tau L{d_{out}}^2/4 \qquad \text{(S2)}$$

where τ is the tortuosity of a curved nanotube, L is the length of a tube (3.4 mm), and d_{s-s} is the interlayer distance of nanotubes (0.35 nm). The τ (1.145) was measured from SEM images.[S1-3]

The porosity of VAMWNTs (φ) was then obtained using the following equations[S1-3]

$$\varphi = \frac{V_A - (\frac{M_A}{M_{VAMWNT}})V_{VAMWNT}}{V_A} \times 100 = \frac{V_A - N_{tubes}V_{VAMWNT}}{V_A} \times 100 \qquad \text{(S3)}$$

where V_A and M_A are the measured volume and mass of the nanotube array. N_{tubes} is the number of nanotubes in the array.[S1-3]

Experimental setup

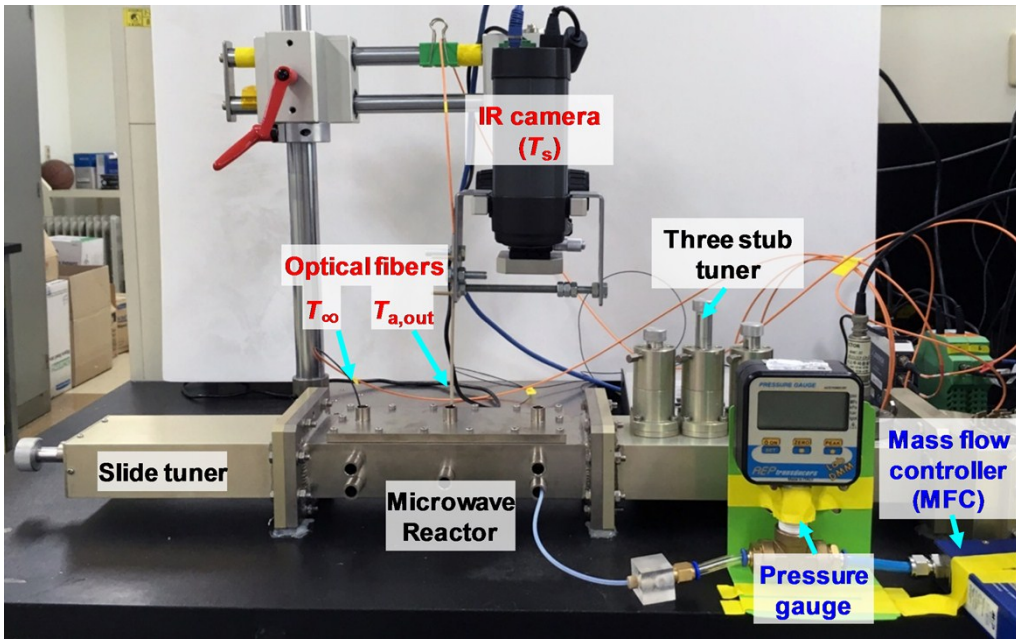

Fig. S1 Experimental setup for the convective heat transfer through the VAMWNT channel.

The single-mode microwave reactor (2.45 GHz) was combined with the gas flow setup. An Infrared (IR) camera and an optical fiber could be switched using a swivel holder, and the temperatures of the outlet surface of the VAMWNT channel (T_s) and the air flowing out of the VAMWNT channel ($T_{a,out}$) were measured at the central port. The ambient air temperature (T_∞) in the reactor was measured at the left port using another optical fiber. The corresponding schematic is provided in Fig. 1c.

Gas flow rate control

A mass flow controller (MFC) was used to control the volumetric flow rate of air through the VAMWNT channel. The indicated volumetric flow rate ($\dot{V}_{STP}$) at the standard temperature and pressure condition (STP, 0 °C and 1 atm) was converted to the volumetric flow rate at a non-STP condition ($\dot{V}_{nSTP}$) based on the mass conservation and ideal gas assumption.[S4]

$$\dot{V}_{nSTP} = \dot{V}_{STP}\frac{P_{STP}T_{nSTP}}{T_{STP}P_{nSTP}} \quad \text{(S4)}$$

where P_{STP} is the pressure at the STP condition (1 atm), T_{nSTP} is the measured air temperature, T_{STP} is the temperature at the STP condition (0 °C), and P_{nSTP} is the measured air pressure. The pressure and temperature were measured at inlet and outlet of the nanotube channel, and mean values were used for P_{nSTP} and T_{nSTP}, respectively.[S5]

The measurement of the VAMWNT emissivity

The emissivity (ε) of the VAMWNTs was measured in accordance with the ASTM standard (E1933-14).[S6] The VAMWNTs were placed on a hot plate heated to 50 ºC. Half of the top surface of the VAMWNTs was covered with 3M insulating tape with a known emissivity (ε = 0.96), and this emissivity was entered into an IR camera software (FLIR, ResearchIR Max). The observed temperature of the surface covered with the tape was recorded. The temperature of the non-covered VAMWNT surface was then monitored. The emissivity was changed until the non-covered VAMWNT surface temperature became equal to the temperature of the 3M tape. This process was repeated three times to obtain the average emissivity of the VAMWNTs (ε = 0.98).

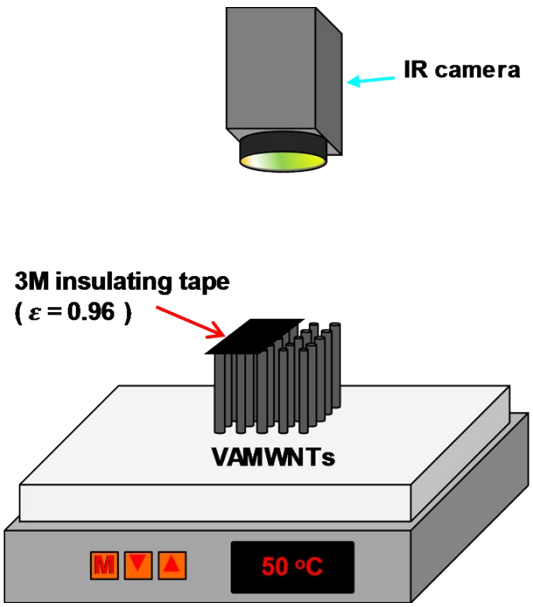

Fig. S2 Schematic of the measurement of the VAMWNT emissivity.

Reproducibility of the temperature measurement of the VAMWNT channel

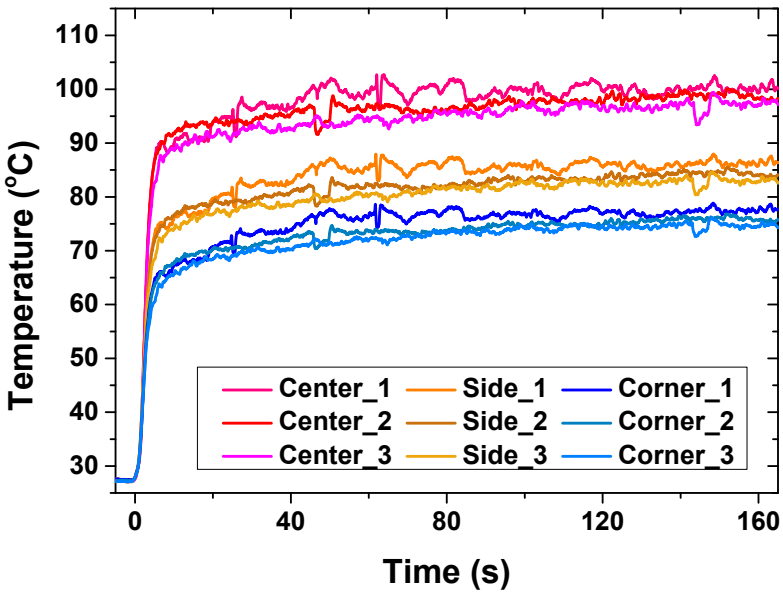

Fig. S3 The outlet surface temperature of the VAMWNT channel was measured 3 times at each condition.

The outlet surface temperature of the VAMWNT channel was measured 3 times at each condition (Fig. S3), and average values were analyzed in main manuscript (Figs. 2 and 3).

Calculation of the volumetric flow rate through the unit cell control volume

The volumetric flow rate through the unit cell control volume ($\dot{V}_{unit\ cell\ control\ volume}$) was calculated by Eq. S5.

$$\dot{V}_{unit\ cell\ control\ volume} = \dot{V}_{nSTP}\frac{A_{c,\ unit\ cell\ control\ volume}}{A_{c,\ VAMWNT\ array}} \quad \text{(S5)}$$

where $A_{c,\ unit\ cell\ control\ volume}$ is the cross-sectional area of the unit cell control volume. $\dot{V}_{nSTP}$ represents the volumetric air flow rate through the entire interstitial space area of the VAMWNTs ($A_{c,\ VAMWNT\ array}$) which is obtained by the product of the tube array porosity (0.983) and the top surface area of the VAMWNTs (5 × 5 mm^2).

Thermophysical properties of air

The temperature-dependent thermophysical properties of air, such as the dynamic viscosity (μ_a), density (ρ_a), specific heat capacity at constant pressure ($C_{p,a}$), and thermal conductivity (k_a), were obtained using following equations [S7, 8]

$$\mu_a = \mu_0\left(\frac{T_0 + 120}{T_{m,a} + 120}\right)\left(\frac{T_{m,a}}{T_0}\right)^{\frac{3}{2}} \quad \text{(S6)}$$

$$\rho_a = \frac{P_{m,a}}{R_A T_{m,a}} \quad \text{(S7)}$$

$$C_{p,a} = 1002.5 + 275 \times 10^{-6}(T_{m,a} - 200)^2 \quad \text{(S8)}$$

$$k_a = 0.02624\left(\frac{T_{m,a}}{300}\right)^{0.8646} \quad \text{(S9)}$$

where T_0 is the reference temperature (291.15 K), μ_0 is the dynamic viscosity of air (18.27 μPa) at T_0, $T_{m,a}$ is the average temperature of air in the channel, $P_{m,a}$ is the average pressure of air in the channel, and R_A is the specific gas constant of air. The pressure and temperature were measured at inlet and outlet of the nanotube channel, and mean values were used for $P_{m,a}$ and $T_{m,a}$.

Slip length calculation

The slip length was calculated by comparing the experimentally measured volume flow rate ($\dot{V}_{unit\ cell\ control\ volume}$) with the Hagen-Poiseuille theory.[S9] Note that the slip length was calculated assuming a flow through a cylindrical channel with the identical D_h. The volume flow rate from the Hagen-Poiseuille theory ($\dot{V}_{HP}$) is expressed by Eq. S10.[S9]

$$\dot{V}_{HP} = \frac{\pi \Delta P}{8\mu_a L \tau} r_h^4 \qquad \text{(S10)}$$

where ΔP is the pressure difference, μ_a is the dynamic viscosity of air, L is the length of the VAMWNTs, τ is the tortuosity of the VAMWNTs, and r_h is the hydraulic radius of the channel. The slip length (L_s) was then calculated by Eq. S11.[S9]

$$L_s = \frac{\dot{V}_{unit\ cell\ control\ volume} - \dot{V}_{HP}}{\frac{4\pi\Delta P}{8\mu_a L \tau} r_h^3} \qquad \text{(S11)}$$

Estimation of the air temperature at the immediate outlet of the VAMWNT channel using the overall heat transfer model

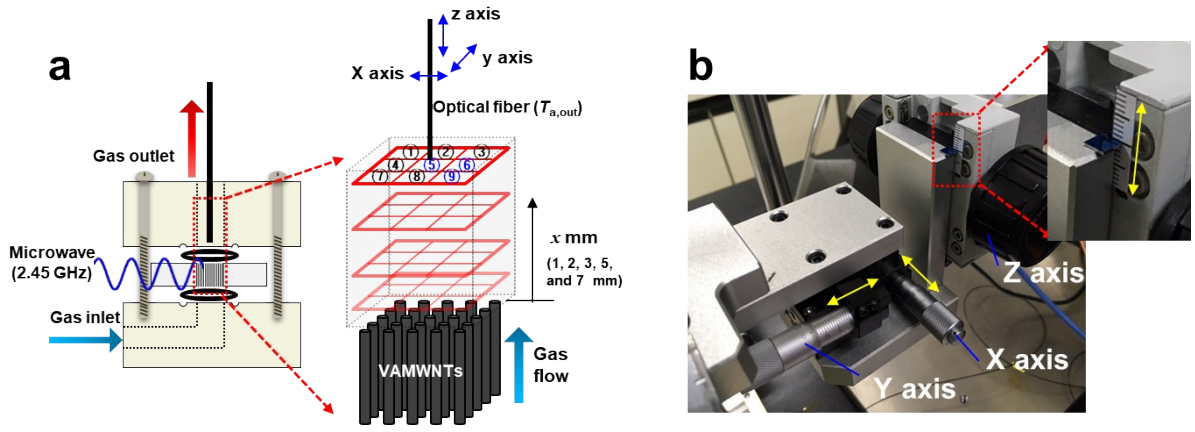

Fig. S4 The air temperature measurement at several different distances from the outlet surface of the VAMWNT channel. **a** Schematic of the experimental setup. **b** Optical image of a three-axis micromanipulator.

As shown in Fig. S4a, the temperature of air was measured at several different distances (1, 2, 3, 5, and 7 mm) from the outlet surface of the VAMWNT channel using an optical fiber temperature sensor. The optical fiber position was adjusted using a three-axis micromanipulator (Fig. S4b), and the air temperature at the center of the gas outlet duct (lateral position 5) was measured. The air cooled down as it flowed along the axial direction of the rectangular gas outlet duct (6 × 6 mm^2) made of polypropylene (PP). The heat transfer of air through the PP channel ($\dot{Q}_{tube}$) was modeled following a previously published protocol, and the schematic of the model is provided in Fig. 3b inset.[S5]

$$\dot{Q}_{tube} = \dot{m}_a C_{p,a}(T_{a,out+x} - T_{a,out}) \qquad \text{(S12)}$$

$$\dot{Q}_{tube} = \bar{U}\, p_{tube}\, x\, \Delta T_{lm} \qquad \text{(S13)}$$

$$\Delta T_{lm} = \frac{\Delta T_{a,out+x} - \Delta T_{a,out}}{\ln(\Delta T_{a,out+x} / \Delta T_{a,out})} \qquad \text{(S14)}$$

where $\dot{m}_a$ is the mass flow rate of air, $C_{p,a}$ is the specific heat capacity of air at constant pressure, $T_{\mathrm{a,out}+x}$ is the air temperature at a distance x from the outlet surface of the VAMWNT channel, $T_{\mathrm{a,out}}$ is the air temperature at the immediate outlet of the VAMWNT channel, U is the overall heat transfer coefficient which includes the combined effect of air convection and conduction across the PP tube wall, p_{tube} is the perimeter of the PP tube, x is the distance from the VAMWNT channel outlet surface, and ΔT_{lm} is the log-mean temperature difference.[S5] $\Delta T_{a,out+x}$ and $\Delta T_{a,out}$ were $T_\infty - T_{a,out+x}$ and $T_\infty - T_{a,out}$, respectively.[S5] The log-mean temperature difference was employed for the model since the ambient air temperature outside of the PP tube wall was constant (T_∞ = 26 ºC) during the experiment (Fig. 3b inset). The final equation was obtained by combining Eqs. S12-S14.[S5]

$$\frac{T_\infty - T_{a,out+x}}{T_\infty - T_{a,out}} = exp(-\frac{p_{tube}\,x}{\dot{m}_a C_{p,a}} U) \qquad \text{(S15)}$$

As shown in Fig. 3b, $T_{\mathrm{a,out}}$ was obtained by fitting the experimental data (temperatures measured at 1, 2, 3, 5, and 7 mm from the outlet surface of the VAMWNT channel) with the model. There was an excellent agreement between the experimental data and the model prediction. This indicated that the temperature measured at the outlet air was not noticeably affected by the carbon nanotube radiation since the model did not consider the radiation effect.

Reynolds number	Heat transfer coefficient (W $m^{-2} K^{-1}$)	Nusselt number	Pressure drop (Pa)	Darcy friction factor
3.82×10^{-5}	4.08×10^{-4}	1.27×10^{-9}	10276	6.87×10^{3}
7.63×10^{-5}	1.02×10^{-3}	3.16×10^{-9}	28286	5.10×10^{3}
1.14×10^{-4}	2.26×10^{-3}	6.94×10^{-9}	47850	4.13×10^{3}
1.51×10^{-4}	3.89×10^{-3}	1.19×10^{-8}	68066	3.56×10^{3}

Table S1. The pressure drop across the VAMWNT channel for the heat transfer condition in Fig. 3e. The Darcy friction factor (f_D) was defined as $\frac{\Delta P}{L} = f_D \cdot \frac{\rho_a}{2} \cdot \frac{v^2}{D_h}$, where ΔP is the pressure drop, L is the channel length, v is the mean flow velocity, and D_h is the hydraulic diameter.[S5] The density of air was measured at inlet and outlet of the nanotube channel, and the mean value was used for ρ_a. The heat flux was 0.286 W m^{-2}.

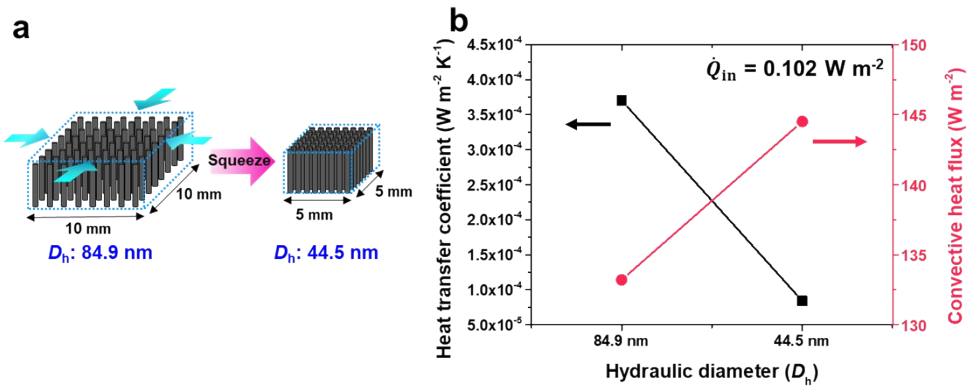

Fig. S5 The effects of the interstitial space on the heat transfer coefficient and convective heat flux (heat flow rate per unit area). **a** The VAMWNTs were synthesized on a larger substrate (10 × 10 mm^2) and squeezed into a lateral dimension of 5 × 5 mm^2. The other synthesis condition was identical to that of the VAMWNTs with D_h = 84.9 nm. **b** The effect of D_h on the h and heat flux. The data of the VAMWNTs with D_h = 84.9 nm were reproduced from Figs. 3e and f for comparison.

REFERENCES

S1. C. Laurent, E. Flahaut and A. Peigney, *Carbon*, 2010, **48**, 2994-2996.

S2. D. Yoon, C. Lee, J. Yun, W. Jeon, B. J. Cha and S. Baik, *ACS Nano*, 2012, **6**, 5980-5987.

S3. W. Jeon, J. Yun, F. A. Khan and S. Baik, *Nanoscale*, 2015, **7**, 14316-14323.

S4. D. Kruh, *Assessment of Uncertainty in Calibration of a Gas Mass Flowmeter*, Springer, Berlin, 2000.

S5. T. L. Bergman and F. P. Incropera, *Fundamentals of Heat and Mass Transfer*, John Wiley & Sons, New York, 2011.

S6. *Standard Practice for Measuring and Compensating for Emissivity Using Infrared Imaging Radiometers*, ASTM International, 2014.

S7. A. J. Smits and J.-P. Dussauge, *Turbulent Shear Layers in Supersonic Flow*, Springer Science & Business Media, Berlin, 2006.

S8. J. C. Dixon, *The Shock Absorber Handbook*, John Wiley and Sons, Chichester, 2007.

S9. J. K. Holt, H. G. Park, Y. Wang, M. Stadermann, A. B. Artyukhin, C. P. Grigoropoulos, A. Noy and O. Bakajin, *Science*, 2006, **312**, 1034-1037.